MedChemComm

CONCISE ARTICLE

View Article Online
View Journal

Cite this: DOI: 10.1039/c5md00127g

Synthesis and *in vitro* antiproliferative activity of novel pyrazolo[3,4-*d*]pyrimidine derivatives†‡

Nermin S. Abdou,[a] Rabah A. T. Serya,*[a] Ahmed Esmat,[b] Mai F. Tolba,[bc] Nasser S. M. Ismail[a] and Khaled A. M. Abouzid[a]

Received 28th March 2015,
Accepted 8th June 2015

DOI: 10.1039/c5md00127g

www.rsc.org/medchemcomm

A novel series of pyrazolo[3,4-*d*]pyrimidine derivatives were designed, synthesized and evaluated for their antiproliferative activity. Among the five compounds selected by NCI, compound **11a** showed a distinctive pattern of selectivity on cell line panels and was further screened for a 5-log dose range, where it showed potent antiproliferative activity with median growth inhibition (GI_{50}) equal to 1.71 μM against the CNS cancer SNB-75 cell line. The tested derivative showed remarkably the highest cell growth inhibition against non-small cell lung cancer HOP-62, CNS cancer SNB-75, breast cancer HS578T, and melanoma MALME-3M cell lines. Flow cytometric analysis revealed that compound **11a** could significantly induce apoptosis in A549 cells *in vitro* at low micromolar concentrations. Further investigation showed that compound **11a** induced significant cell cycle arrest at G0/G1 phase partly due to its ability to downregulate cyclin D1 and upregulate $p27^{kip1}$ levels.

1 Introduction

Cancer is an enormous global health burden, touching every region and socio-economic level. It is the second major cause of death worldwide, exceeded only by heart disease.[1] Extensive efforts are being carried out in order to discover new treatments but despite improved imaging, molecular diagnostic techniques, and advances in prevention and chemotherapeutic management, the disease still affects many millions of patients worldwide[2,3] and no complete cure has been discovered. Apart from surgical treatment and irradiation techniques, chemotherapy still remains an important option for cancer therapy; unfortunately, the treatment of most types of solid tumors (*e.g.* breast and ovarian) is still a problem and survival rates remain significantly low.[4]

Finding safe and effective anticancer agents is still one of the hardest challenges in the field of drug discovery.

Pyrazolo[3,4-*d*]pyrimidine derivatives demonstrate various biological activities, such as inhibition of phosphodiesterase-5 (PDE-5),[5] modulation of the human adenosine receptor,[6] antiviral,[7] anticoccidial,[8] antimicrobial,[9] *etc.* These investigations revealed that substitution of various groups on the ring imparts different activities.[5–9]

The pyrazolo[3,4-*d*]pyrimidine scaffold can be considered as a bioisostere of the ATP purine ring, and hence may exhibit promising antitumor activity by acting as a competitive ATP inhibitor of many kinase enzymes. Fig. 1 illustrates the similarity between the ATP structure and different reported pyrazolo[3,4-*d*]pyrimidine derivatives as antitumor agents.[10–13]

Angiogenesis is the formation of new blood vessels, and is an essential process for tumor growth. The selective inhibition of tumor angiogenesis might be a useful strategy for inhibiting tumor growth and metastasis. Vascular endothelial growth factor (VEGF) is an important regulator of vascular growth and permeability. Overexpression of VEGF in solid tumors has been shown to promote angiogenesis, thereby facilitating tumor growth. VEGF acts on VEGF-R2, a receptor tyrosine kinase present on the surface of endothelial cells. The inhibition of VEGF-R2 by small molecules is a validated therapeutic approach for treatment of cancer and has received much attention in the literature.[14]

In this study, we report the design, synthesis and biological evaluation of pyrazolo[3,4-*d*]pyrimidine derivatives as target antiproliferative agents.

Our basic design strategy for new scaffolds acting as antiproliferative agents was based on the following:

1. The pyrazolo[3,4-*d*]pyrimidine scaffold was chosen as it is considered to be an isostere of purine and hence may

[a] *Pharmaceutical Chemistry Department, Faculty of Pharmacy, Ain Shams University, Cairo 11566, Egypt. E-mail: rabahat2003@yahoo.com, khaled.abouzid@pharma.asu.edu.eg; Tel: +20 2 01229415877*
[b] *Department of Pharmacology & Toxicology, Faculty of Pharmacy, Ain Shams University, Cairo 11566, Egypt*
[c] *Biology Department, School of Sciences and Engineering, The American University in Cairo, New Cairo, Egypt*

† The authors declare no conflict of interest.

‡ Electronic supplementary information (ESI) available. See DOI: 10.1039/c5md00127g

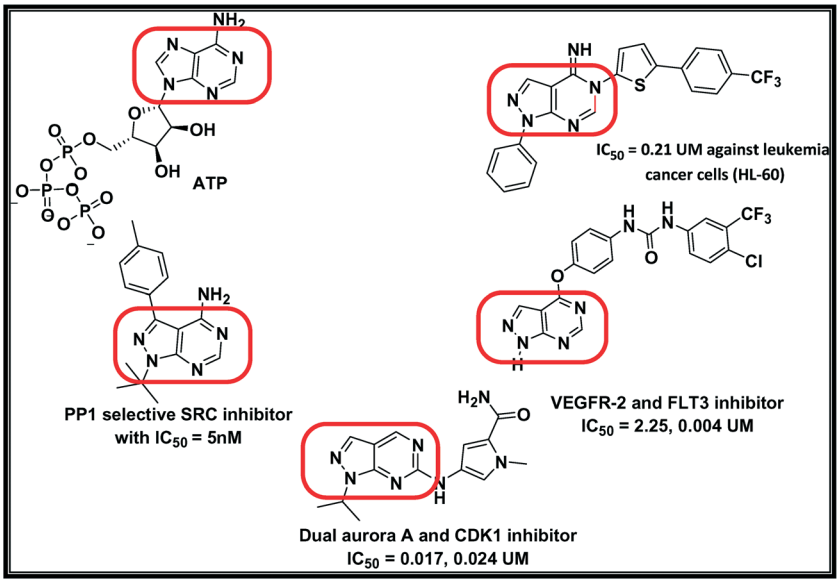

Fig. 1 Structures of ATP and different reported biologically active compounds containing the pyrazolo[3,4-*d*]pyrimidine scaffold imparting different mechanisms as antitumor agents.

exhibit promising antitumor activity by acting as a competitive ATP inhibitor of many kinase enzymes.

2. Exploration of previously revealed SAR studies and bioisosteric modifications of reported lead compounds.[15–20]

The target compounds were originally designed to act as VEGFR inhibitors through the following considerations:

1. The main scaffold occupying the ATP binding site can be replaced with a substituted pyrazolo[3,4-*d*]pyrimidine scaffold.

2. The linker can be urea, amide, or ether.

3. The aryl moiety, essential for allosteric site binding, is to be conserved either substituted or not.

The target compounds (series 1–5) were rationally designed based on the bioisosteric modifications of the reported lead VEGFR inhibitors as illustrated in Fig. 2.

2 Results and discussion

2.1. Chemistry

The synthetic approaches adopted to obtain the different derivatives (**7a–e**, **9a–d**, **11a–f**, and **13a–d**) are outlined in Schemes 1–5.

The general synthetic route to 4-chlorophenyl-1*H*-pyrazolo[3,4-*d*]pyrimidine **1a** and 4-chloro-1-chlorophenyl-1*H*-pyrazolo[3,4-*d*]pyrimidine **1b** has been outlined in Scheme S1 (*c.f.* ESI‡). The pyrazoles were cyclized to pyrazolo[3,4-*d*]pyrimidine by refluxing in formamide,[21,22] then the 4-chloro derivatives were prepared by chlorination with phosphorus oxychloride.[23]

In Scheme 1, the 4-amino diphenyl urea derivatives **2b–e** were synthesized in 2 steps first by reacting 4-nitroaniline with the appropriate aryl isocyanate in methylene chloride,[24] then reduction of the produced 4-nitro derivative using stannous chloride dihydrate.[25] The target products **3a–e** were prepared in moderate to high yields from the reaction of the chloro derivatives **1a** and **b** with the appropriate amines **2b–e**.

4-Hydroxy diphenyl urea derivatives were synthesized from phenyl isocyanate by reaction with 4-aminophenol in dioxane according to the reported procedures,[26] and then the hydroxy derivative was reacted with the chloro derivatives **1a** and **b** to give target compounds **4a** and **b**.

The synthetic route which was attempted to synthesize 6-nitro-2,3-dihydrobenzo[*d*]thiazol-2-one started with cyclization of 4-nitroaniline to 6-nitro-2-amino-2,3-dihydrobenzo[*d*]thiazole under standard conditions,[27] followed by diazotization and hydrolysis in acidic medium[28] to give the intermediate 6-nitro-3*H*-benzothiazol-2-one in an overall low yield (26%). Alkylation of 6-nitro-3*H*-benzothiazol-2-one to give the corresponding *N*-alkylated intermediates **5a–d** was conducted in a KOH/acetone/water mixture using appropriate aralkyl halides under reflux conditions[29] to obtain the desired intermediates in an excellent yield.

Reduction of the *N*-alkylated intermediates **5a–d** was carried out under standard conditions reported by Abdelaal *et al.*[28] using 10% Pd/C and hydrogenation at 35 psi to give the corresponding amines **6a–d**. Carrying out the reduction in ethanol/THF at a ratio of 3 : 1 improved the yield dramatically. The target compounds **7a–e** were finally obtained from the reaction of the amines **6a–d** and the chloro intermediates **1a** and **b** in ethanol under reflux with the addition of few drops of triethylamine.

Compounds **9a–d** were also prepared in the same way from the reaction of amines **8a** and **b** and the chloro intermediates **1a** and **b** under the same conditions. The synthesis of these compounds was outlined in Scheme 3.[25]

In order to synthesize compounds **11a–f**, the steps illustrated in Scheme 4 were adopted. First, *p*-nitrobenzoyl

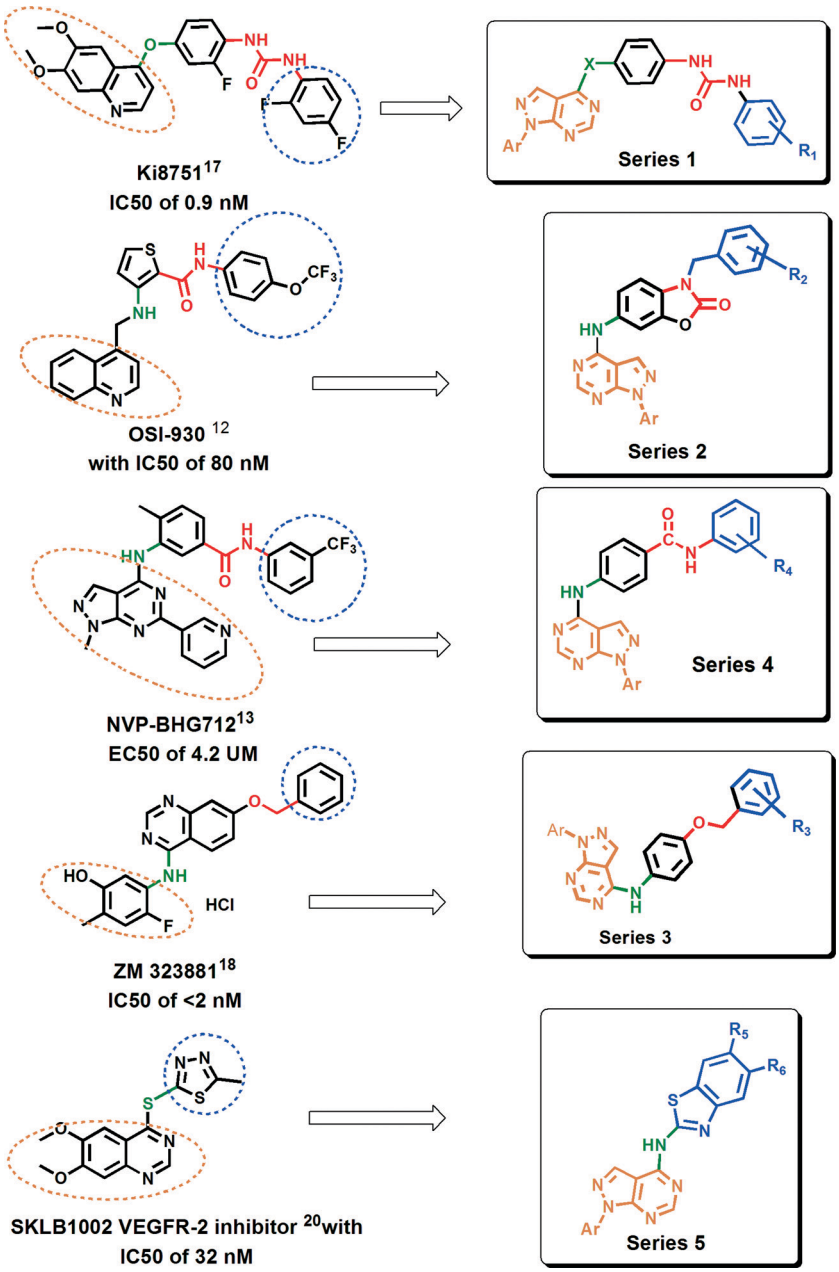

Fig. 2 Rational design of the target compounds (series 1–5).

chloride was obtained from the corresponding acid using thionyl chloride under reflux conditions as reported,[30] which was then reacted with different amines in DCM in the presence of triethylamine in a typical amide formation to give the amide derivatives.[31] The amide derivatives were reduced using stannous chloride dihydrate to produce amino derivatives **10a–d**.[32] Compounds **11a–f** were obtained by the reaction of the amino derivatives **10a–d** with compounds **1a** and **b** in ethanol under reflux followed by purification of the resulting precipitate. Finally, compounds **13a–d** were obtained by reacting commercially available benzothiazolamines **12a–c** and the chloro derivatives **1a** and **b** under the same conditions (Scheme 5).

2.2. Biological evaluation

2.2.1. VEGFR-2 enzyme inhibition assay. The aim of this study was to identify whether any of the compounds can affect the activity of VEGFR-2 tyrosine kinase. The percent change of the enzymatic activity was evaluated against a reference kinase inhibitor control at 10 μM. The results observed as % activity change compared to that of the control are presented in Table S1 (*c.f.* ESI‡), and the intra-assay variability was determined to be less than 10%. Inhibition of target activity by the compounds gives negative (−) values while activation of target activity gives positive (+) values. Unfortunately, the profiling data for the compounds tested against VEGFR-2 showed insignificant enzyme inhibition. In the light

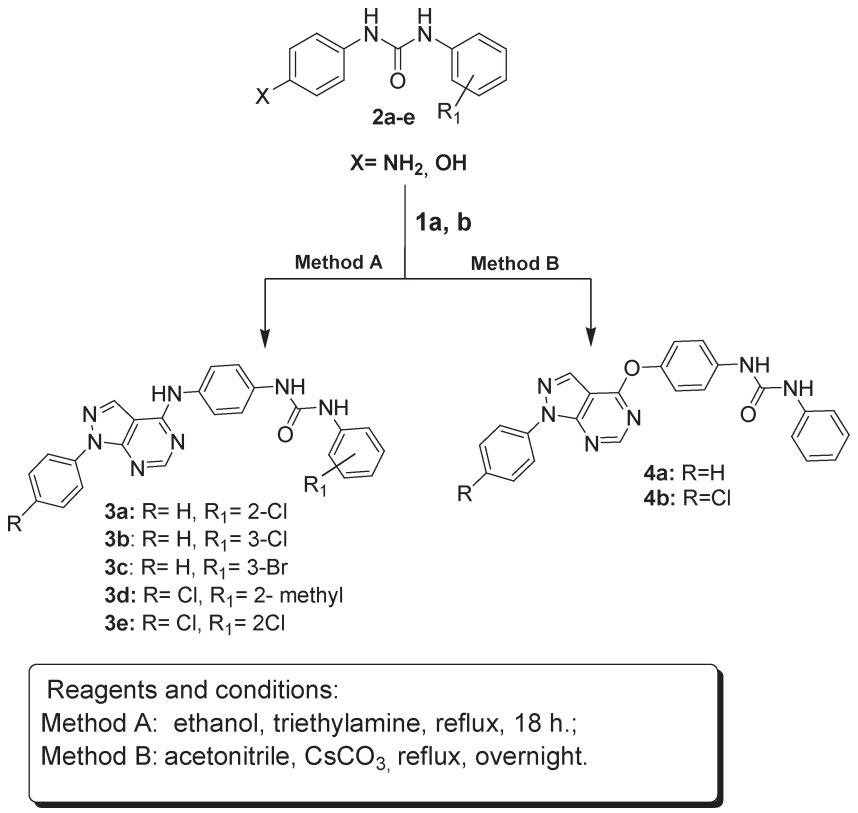

Scheme 1 Synthesis of **3a–e** and **4a** and **b**.

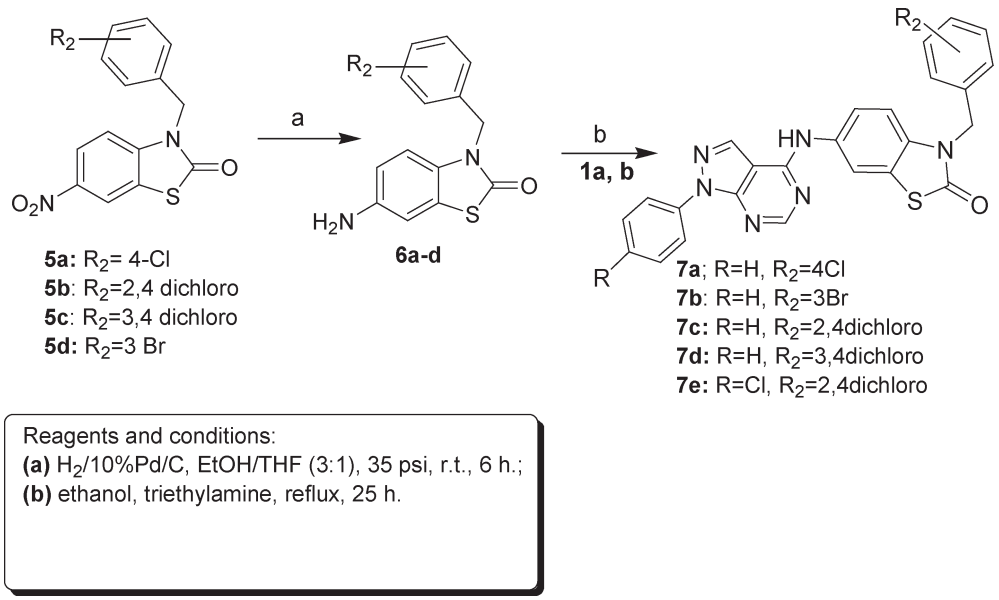

Scheme 2 Synthesis of **7a–e**.

of this information, further investigation was conducted to evaluate the antiproliferative activities of the synthesized compounds as demonstrated next.

2.2.2. Antiproliferative activity

2.2.2.1. Anticancer screening at NIH, Bethesda, Maryland, USA. All the prepared final compounds were submitted to the National Cancer Institute "NCI" (www.dtp.nci.nih.gov); five compounds (**7a**, **9a**, **9c**, **11a**, and **13a**) were selected under the Developmental Therapeutic Program (DTP). The operation of this screening utilizes 60 different human tumor cell lines, representing leukemia, melanoma, and cancers of the lung, colon, brain, ovary, breast, prostate, and kidney. Selection for

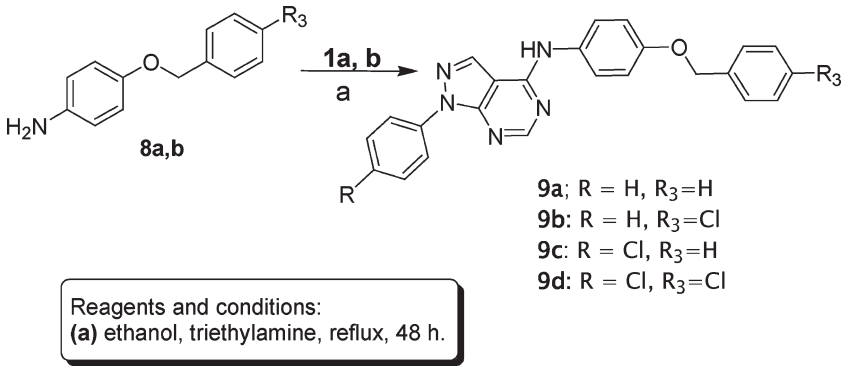

Scheme 3 Synthesis of **9a–d**.

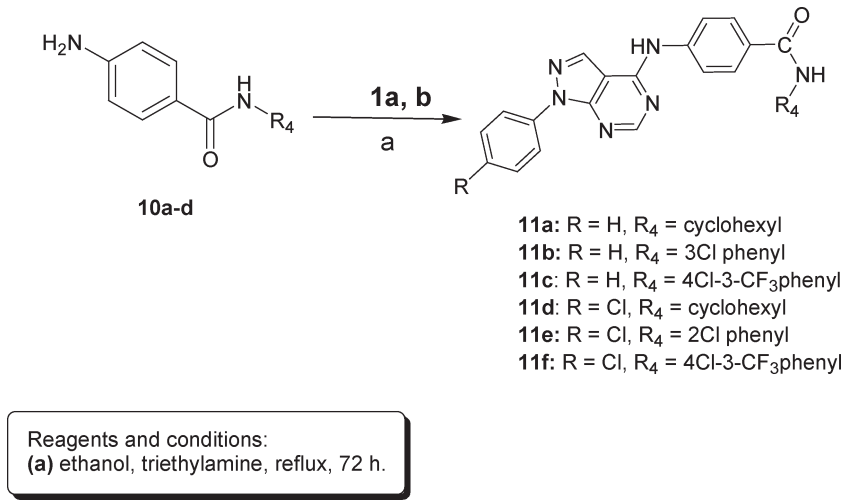

Scheme 4 Synthesis of **11a–f**.

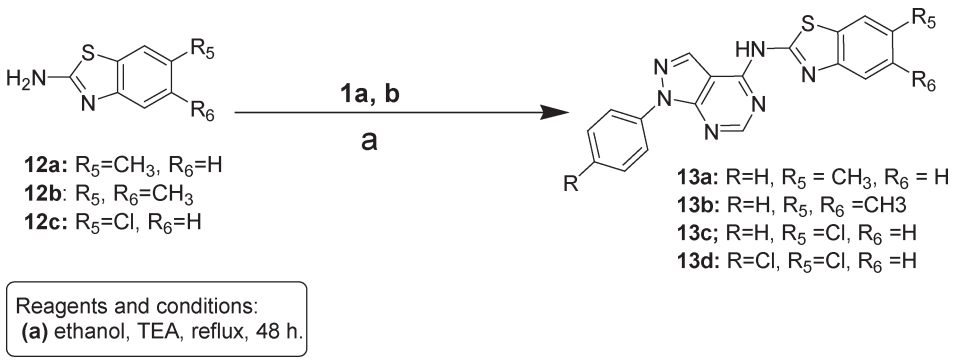

Scheme 5 Synthesis of **13a–d**.

screening is based on the ability of the submitted compounds to add diversity to the NCI small molecule compound collection. All selected compounds with NCI codes NSC 775949/1, NSC 775947/1, NSC 775950/1, NSC 775951/1, and NSC 775948/1 were tested at a single dose (10 μM) in the full NCI 60-cell panel. Among the five selected compounds, compound **11a** (NSC 775951/1) was further screened for the 5-log dose molar range as it has shown prominent cell growth inhibition at 10 μM against a variety of cell lines.

2.2.2.1.1. Primary in vitro single dose screening of anticancer activity in full NCI 60-cell line panel. Primary *in vitro* one dose (10 μM) anticancer activity screening was performed in a full NCI 60-cell panel. The results for each compound were reported as a mean graph of the percent growth of the treated cells compared to that of the untreated

control cells. The mean graph of **11a** produced from the NCI 60-cell line screening program is illustrated in Fig. S1 (*c.f.* ESI‡).[34] This primary screening indicated that compound **11a** possesses higher selectivity against non-small cell lung cancer and CNS cancer cells with mean growth inhibition percentages of 73.56 and 62.91%, respectively. Compound **11a** showed remarkable cell growth inhibition at 10 μM against a variety of cell lines as highlighted in Table 1, which prompted the 5-dose study to be carried out.

The cell growth percentages of the target compounds (**7a**, **9a**, **9c**, **11a**, and **13a**) against the full 60-cell line panel are presented in Table 1.

In light of the NCI 60-cell line screening results, the following observations could be made:

• Compound **7a** showed good antiproliferative activity against renal A498 and UO-31 cancer cell lines with cell growth inhibition percentages of 41.05% and 49.27%, respectively. Cell growth inhibition was also high for the prostate PC-3 cancer cell line (44.4%) and leukemic K-562 cell line (50.44%).

• Compound **13a** showed good antiproliferative activity against the leukemic SR cell line with a cell growth inhibition percentage of 55.18%, as well as the non-small cell lung cancer NCI-H322M cell line with an inhibition percentage of 54.33%.

• Compound **11a** exhibited a prominent cell growth inhibitory effect in most of the tested cell lines as demonstrated in Table 1.

2.2.2.1.2. In vitro five dose full NCI 60-cell panel assay. Compound **11a** (NSC 775951/1) was selected for further screening at five different concentrations (0.01, 0.1, 1, 10, and 100 μM) as it showed the most prominent cell growth inhibition at 10 μM concentration against a variety of cell lines. The assay results were used to create log concentration *vs.* % growth curves and three response parameters namely GI_{50} (median growth inhibition), TGI (total growth inhibition = cytostatic activity), and LC_{50} (median lethal growth inhibition = cytotoxic activity) were calculated in μM for each cell line.[33] The results are shown in Fig. S2 and S3 (*c.f.* ESI‡) and Table 2. Compound **11a** exhibited remarkable anticancer activity against most of the tested cell lines representing nine different subpanels. GI_{50} values were between 1.71–23.9 μM, except for five cell lines of different subpanels namely leukemic cell line MOLT-4, colon cancer cell lines HCT-15 and KM12, melanoma cell line MDA-MB-435, and breast cancer cell line MCF7 showing GI_{50} values up to 75.6, 99.3, 57.8, 67.8 and 74.1 μM, respectively (Table 2).

With regard to the sensitivity against some individual cell lines (Table 2), compound **11a** showed remarkable activity against the CNS SNB-75 cancer cell line with a GI_{50} value of 1.71 and a TGI value of 5.40 and the melanoma MALME-3M cell line with a GI_{50} value of 1.97 and a TGI value of 4.94.

The collective dose response curve and individual dose response curves of all cell lines tested are shown in Fig. S2 and S3 (*c.f.* ESI‡), respectively.

The criterion for the selectivity of a compound depends on the ratio obtained by dividing the full panel MID (the

Table 1 Percentage of cell growth of NCI 60 cancer cell lines displayed by the final compounds (**7a**, **9a**, **9c**, **11a**, and **13a**)

Panel/cell line	Percentage cell growth				
	7a	**9a**	**9c**	**11a**	**13a**
Leukemia					
CCRF-CEM	63.56	80.79	78.92	64.93	87.87
HL-60 (TB)	66.90	99.77	86.89	106.24	103.14
K-562	*49.56*[b]	90.33	87.28	73.17	102.24
MOLT-4	*58.59*[b]	93.07	89.56	89.52	102.43
RPMI-8226	63.51	96.50	86.36	89.53	101.97
SR	80.64	91.95	83.27	67.48	*44.82*[b]
Non-small cell lung cancer					
A549/ATCC	78.01	104.13	88.76	*16.57*[b]	101.75
HOP-62	93.96	103.51	81.58	*−66.54*[b]	110.16
HOP-92	64.36	98.79	97.82	*37.74*[b]	97.54
NCI-H226	71.44	103.08	101.76	*19.13*[b]	100.78
NCI-H23	84.73	108.51	92.70	72.04	106.46
NCI-H322M	75.65	84.12	75.01	63.97	*45.67*[b]
NCI-460	83.52	93.68	93.09	*42.17*[b]	98.37
Colon cancer					
COLO 205	92.69	107.01	91.21	65.37	109.89
HCC-2998	NT[a]	108.06	98.03	NT[a]	105.79
HCT-116	80.29	106.36	94.82	*37.65*[b]	99.36
HCT-15	86.45	72.41	87.15	66.58	97.82
HT29	106.36	115.50	84.65	70.23	103.33
KM12	71.63	98.25	80.16	88.49	98.87
SW-620	84.39	98.71	100.85	72.91	100.20
CNS cancer					
SF-268	85.57	108.02	99.67	*36.92*[b]	114.14
SF-295	87.16	107.12	97.83	73.36	99.85
SF-539	79.19	99.64	92.44	*43.72*[b]	101.04
SNB-19	85.63	95.97	NT[a]	*48.73*[b]	98.25
SNB-75	88.34	102.49	86.37	*−20.35*[b]	106.68
U251	96.64	105.58	94.99	*40.19*[b]	102.73
Melanoma					
MALME-3M	86.42	92.76	85.12	*2.93*[b]	87.04
M14	82.85	101.33	93.61	69.10	106.94
MDA-MB-435	84.19	90.10	83.23	81.16	91.92
SK-MEL-2	87.97	115.23	NT[a]	79.10	108.80
SK-MEL-28	90.10	95.95	90.43	62.24	95.29
SK-MEL-5	87.25	94.27	94.40	75.43	92.06
UACC-257	92.57	120.63	101.77	*56.48*[b]	111.92
UACC-62	*58.26*[b]	93.28	104.81	63.86	94.68
Ovarian cancer					
IGROV1	81.82	100.04	101.96	71.12	99.59
OVCAR-3	86.60	112.54	101.52	87.44	108.46
OVCAR-4	86.98	91.33	80.57	*30.27*[b]	103.78
OVCAR-5	75.11	98.93	92.84	80.27	96.04
OVCAR-8	87.92	113.12	97.95	*21.63*[b]	107.04
NCI/ADR-RES	84.79	107.36	94.55	74.18	105.64
SK-OV-3	100.62	107.57	99.73	*54.02*[b]	111.66
Renal cancer					
786-0	93.69	100.45	102.91	72.06	103.25
A498	*58.95*[b]	77.87	85.22	*50.40*[b]	66.37
ACHN	74.61	103.91	98.61	*54.27*[b]	106.72
CAKI-1	71.58	99.06	93.66	62.29	102.89
RXF-393	79.54	101.80	97.85	62.16	98.96
SN12C	75.01	97.38	NT[a]	*18.96*[b]	97.55
TK-10	104.89	111.11	92.14	*50.98*[b]	117.68
UO-31	*50.73*[b]	79.60	83.61	*57.72*[b]	91.72
Prostate cancer					
PC-3	*55.60*[b]	88.50	86.08	*53.30*[b]	98.26
DU-145	94.54	103.66	100.20	*54.57*[b]	103.47
Breast cancer					
MCF7	85.26	100.50	95.89	82.83	97.21
MDA-MB-231/ATCC	57.73	101.04	NT[a]	*8.76*[b]	102.21
HS 578T	81.13	109.14	96.61	*0.22*[b]	120.22
BT-549	100.94	106.45	106.74	*59.80*[b]	107.58
T-47D	62.31	100.20	82.52	76.80	107.55

Table 1 *(continued)*

Panel/cell line	Percentage cell growth				
MDA-MB-468	65.93	93.06	91.50	76.06	80.31

[a] NT: not tested. [b] Italicized values represent those below 60.00% growth.

average sensitivity of all cell lines toward the test agent) by their individual subpanel MID (the average sensitivity of all cell lines of a particular subpanel toward the test agent). Ratios between 3 and 6 refer to moderate selectivity, and ratios greater than 6 indicate high selectivity toward the corresponding cell line, while compounds not meeting either of these criteria are rated as non-selective.[35] As per this criterion, compound **11a** in this study was found to be highly selective toward CNS cancer with a selectivity ratio of 8.25 and moderately selective toward non-small cell lung, renal and ovarian cancer subpanels only with selectivity ratios of 4.51, 3.16 and 3.11, respectively, whereas it was found to be non-selective against the remaining cell panels (Table 2).

*2.2.2.1.3. Effects of compound **11a** on the cell cycle.* Compound **11a** was further investigated for its possible mechanisms of anticancer activity using non-small cell lung cancer cells based on the selectivity ratio drawn from the NCI results. The cytotoxicity assay at 5 different concentrations (0.1, 1, 10, 100, and 1000 μM) was repeated under our laboratory conditions using sulforhodamine-B (SRB) and the IC_{50} in the A549 cell line was 66.6 μM (Fig. 3). Exposure of A549 lung cancer cells to compound **11a** at a concentration equal to its IC_{50} for 48 h induced a significant ($P < 0.001$) increase in the percentage of cells at G0/G1 phase by about 11.9% compared to the untreated cells (Fig. 4). This could partly explain the antiproliferative activity of compound **11a**.

*2.2.2.1.4. Effects of compound **11a** on cell cycle regulatory molecules.* The significant cell cycle arrest induced by compound **11a** at G0/G1 phase was further substantiated through assessing the expression levels of two cell cycle regulatory molecules cyclin D1 and $p27^{kip1}$ that are known to regulate the transition at this phase of the cell cycle. Hall and Peters previously demonstrated that cyclin D1 levels are unregulated in several types of tumors including NSCLC.[36] Treatment of A549 cells with compound **11a** triggered a significant reduction in the protein abundance of the cell cycle inducer cyclin D1 by about 51% compared to control cells as shown by immunocytochemistry (Fig. 5). Cyclin D1 expression is known to be maintained through G1 phase as it is required for the transition of cells to S phase where its levels decline again to allow for DNA synthesis.[37] Therefore, the evidenced reduction in cyclin D1 abundance after treatment with compound **11a** can justify the cell cycle arrest at G0/G1 phase. p27/Kip1 is a member of the Cip/Kip family of cyclin-dependent kinase inhibitors. They function *via* forming heterotrimeric complexes with cyclins and CDKs, with subsequent inhibition of kinase activity and blockage of progression through G1/S phase.[38] In the current study, treatment of A549 cells with compound **11a** significantly boosted the protein expression of the cell cycle inhibitor $p27^{kip1}$ by about 3 folds (Fig. 6). To sum up, compound **11a** induced cell cycle arrest at G0/G1 phase and this could be at least partly due to its ability to downregulate cyclin D1 and upregulate $p27^{kip1}$ levels.

2.2.2.2. Antiproliferative activity against MCF-7 human breast cancer cell line. The rest of the synthesized compounds (**3a–e**, **4a** and **b**, **7b–e**, **9b** and **d**, **11b–f**, and **13b–d**) not chosen by NCI were screened for their cytotoxic activity against MCF-7 (breast) human tumor cell line utilizing the *in vitro* sulforhodamine-B (SRB) standard method.[33] Doxorubicin, which is one of the most effective anticancer agents, was used as the reference drug in this study. The relationship between the surviving fraction and drug concentration was plotted to obtain the survival curve of the breast cancer cell line (MCF-7). The response parameter calculated was the IC_{50} value, which corresponds to the concentration required for 50% inhibition of cell viability. Table 3 shows the *in vitro* cytotoxic activity of the synthesized compounds; it is apparent that most of the synthesized analogs exhibit good antiproliferative properties against the tested human tumor cell line. However, compound **11b** exhibited more potent cytotoxic effects compared to the reference compound doxorubicin with IC_{50} values of 1.12 and 1.172 μM, respectively. Moreover, there are six compounds that showed significant antitumor activity.

We can conclude from these results (Table 3) the structure–activity correlation of the synthesized compounds with the following observations:

► The pyrazolo[3,4-*d*]pyrimidine ring is a suitable backbone for cytotoxic activity.

► Both the amide and thiazole series displayed considerable potency.

► The cytotoxicity of the alkylated thiazolone and urea series depends on different substituents.

► The introduction of *p*-chloro in the phenyl moiety at the N-1 position of pyrazolopyrimidine affects the activity dramatically; it may increase or decrease the cytotoxic activity which might be due its effect on the length of the conformation adopted by the compound.

2.3. Enzyme inhibition assay

This assay was performed to determine whether any of the compounds can modulate the activity of the protein kinase targets identified from comparative analysis and target fishing. The percent change of the enzymatic activity produced by the synthesized compounds against EGFR, Aurora-A, SRC, P38α, C-MET, PDGFR and HER2 kinases was evaluated against a reference kinase inhibitor control at 10 μM (Table S2, *c.f.* ESI‡).

The profiling data for the compounds tested against EGFR, Aurora-A, SRC, P38α, C-MET, PDGFR and HER2 showed weak inhibition of some protein kinase targets by a few compounds. The results of EGFR activity showed weak

Table 2 NCI *in vitro* testing results for compound **11a** (NSC 775951/1) at five-dose levels in μM

Panel/cell line	GI_{50}(μM)	SubpanelMID[b]	Selectivity ratio(MID[a] : MID[b])	TGI(μM)	LC_{50}(μM)
Leukemia		71.8	0.41		
CCRF-CEM	>100			>100	>100
MOLT-4	75.6			>100	>100
RPMI-8226	>100			>100	>100
SR	11.6			49.1	>100
Non-small cell lung cancer		6.63	4.51		
A549/ATCC	*4.38*			51.3	>100
HOP-62	*2.62*			8.78	37.3
HOP-92	*2.53*			8.29	86.6
NCI-H226	*3.35*			21.5	>100
NCI-H23	10.9			89.9	>100
NCI-H322M	15.8			>100	>100
NCI-460	*7.09*			>100	>100
NCI-H522	*6.40*			>100	>100
Colon cancer		62.26	0.48		
COLO 205	12.5			>100	>100
HCT-2998	>100			>100	>100
HCT-116	*4.01*			>100	>100
HCT-15	99.3			>100	>100
KM12	57.8			>100	>100
SW-620	>100			>100	>100
CNS cancer		3.63	8.25		
SF-268	*5.85*			>100	>100
SF-295	*2.98*			13.3	43.1
SF-539	*3.81*			17.1	49.0
SNB-19	*3.82*			18.9	>100
SNB-75	*1.71*			5.40	35.9
Melanoma		17.27	1.73		
LOX IMVI	*4.49*			22.3	>100
MALME-3M	*1.97*			4.94	21.0
M14	18.3			>100	>100
MDA-MB-435	67.8			>100	>100
SK-MEL-2	13.6			36.2	96.3
SK-MEL-28	3.79			>100	>100
SK-MEL-5	21.7			>100	>100
UACC-257	*6.42*			>100	>100
UACC-62	17.4			>100	>100
Ovarian cancer		9.63	3.11		
IGROV1	14.4			65.9	>100
OVCAR-3	14.3			>100	>100
OVCAR-5	15.2			95.2	>100
OVCAR-8	*3.87*			19.3	>100
NCI/ADR-RES	*7.06*			>100	>100
SK-OV-3	*2.95*			8.70	51.1
Renal cancer		9.46	3.16		
786-0	*3.47*			18.3	65.5
A498	*3.83*			39.4	>100
ACHN	*3.32*			11.0	37.0
CAKI-1	14.0			>100	>100
RXF-393	*2.43*			9.33	56.9
SN12C	*8.26*			>100	>100
TK-10	16.5			49.5	>100
UO-31	23.9			>100	>100
Prostate cancer		11.2	2.67		
PC-3	11.8			44.8	>100
DU-145	10.6			48.1	>100
Breast cancer		21.69	1.38		
MCF7	74.1			>100	>100
MDA-MB-231/ATCC	*5.09*			21.9	80.6
HS 578T	*3.37*			34.2	>100
BT-549	*5.69*			26.4	91.9
T-47D	20.2			>100	>100
MDA-MB-468	21.7			>100	>100
		29.96			

Italicized values represent those GI_{50} values which are less than 10 μM. [a] MID = Average sensitivity of all cell lines in μM. [b] MID = Average sensitivity of all cell lines of a particular subpanel in μM.

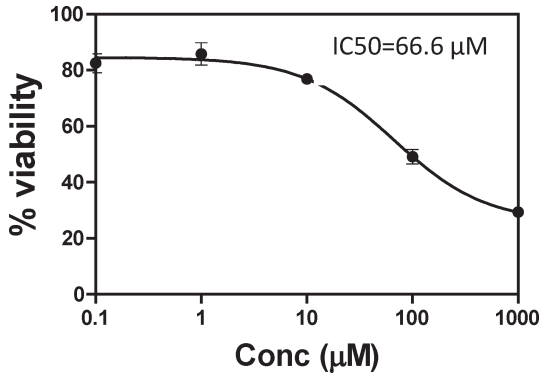

Fig. 3 Concentration–response curve of compound **11a** (N) in A549 non-small cell lung cancer cells. Cells were exposed to 5 different concentrations (0.1, 1, 10, 100, and 1000 μM) of the tested agent for 72 h and then cell viability was determined using SRB assay. Data are mean ± SD (n = 3). Experiments were carried out in triplicate.

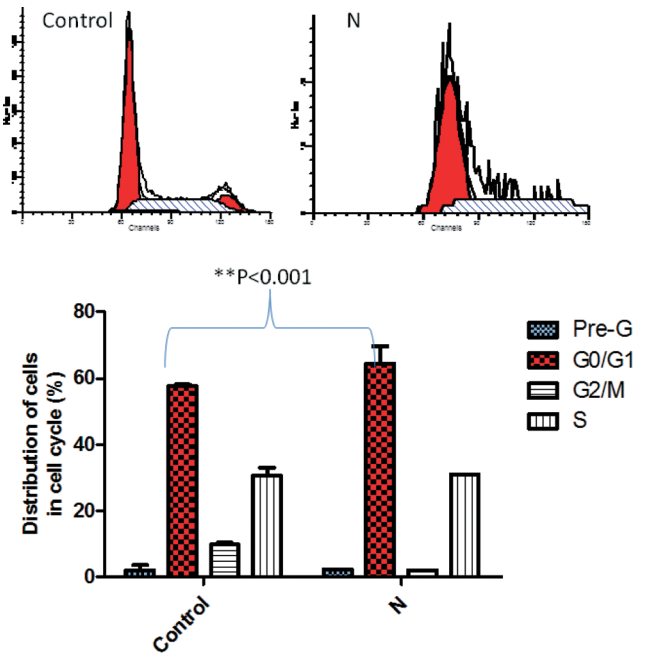

Fig. 4 Effect of compound **11a** (N) on DNA-ploidy flow cytometric analysis of A549 cells. The cells were treated with compound **11a** (25 mM) for 48 h. Data are mean ± SD (n = 3). Experiments were carried out in triplicate.

inhibition by two compounds (**11b** and **13a**) while those for Aurora-A showed weak inhibition by one compound (**3b**). Weak inhibition by **7a** was also shown for the protein kinase target PDGFR.

2.4. ADMET studies

Computer-aided ADMET studies were performed by using the software Accord for Excel (Accelrys Discovery Studio 2.5 software). These studies are solely based on the chemical structure of the molecule. Some of the parameters that are

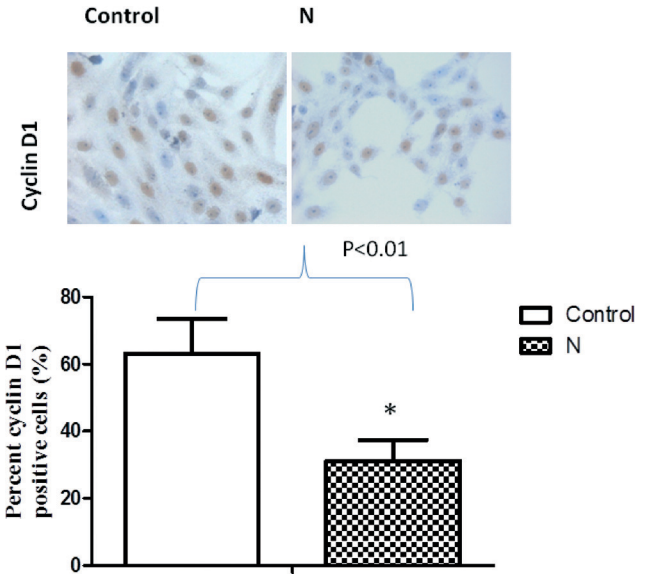

Fig. 5 The effect of compound **11a** (N) on the protein abundance of cyclin D1 in A549 cells assessed through immunocytochemistry. Data are mean ± SD (n = 3). Experiments were carried out in triplicate.

calculated using Accord for Excel include atom based log P98 (A log P98),[39] ADMET 2D polar surface area (ADMET 2D PSA), aqueous solubility (AQ SOl), aqueous solubility level (AQ SOl LEV), blood brain barrier value (BBB), blood brain barrier level (BBB LEV), cytochrome P450 2D6 (CYP2D6), cytochrome P450 2D6 probability (CYP PROB), hepatotoxicity level (HEPATOX LEV), hepatotoxicity probability (HEPATOX PROB), plasma protein binding logarithmic value (PPB LOG) and plasma protein binding logarithmic level (PPB LEV).

The structures of the compounds were drawn using DS ViewerPro Suite software and appended to Accord for Excel software, then the parameters were calculated.

2.4.1. Results of ADMET studies. All the parameters calculated are tabulated in Table 4. The ADMET plot is a 2D plot generated using calculated PSA_2D and A log P98 properties.

Blood Brain Barrier (BBB) and Human Intestinal Absorption (HIA) plots (Fig. 7) were drawn using all the compounds.

In the BBB plot, 19 compounds fall outside the 99% ellipse (undefined). Hence, these compounds may not be able to penetrate the blood brain barrier, and the chances of CNS side effects are low or absent. On the contrary, seven compounds from the benzyloxy and benzothiazole series, and the cyclohexylamide (**11a**) compound lie inside the 99% ellipse, thus they have a medium to high degree of penetration.

In the HIA plot, seven compounds fall outside the 99% confidence ellipse (undefined), whereas the remaining compounds fall inside the 99% ellipse. Hence, compounds **4a**, **9a**, **11a** and **b**, and **13a–c** are expected to possess good human intestinal absorption. Compound **7e** shows very low absorption as it contains three chloro groups. The ADME aqueous solubility logarithmic level of most of the compounds was found to be 2, 1 or 0 which indicates very low

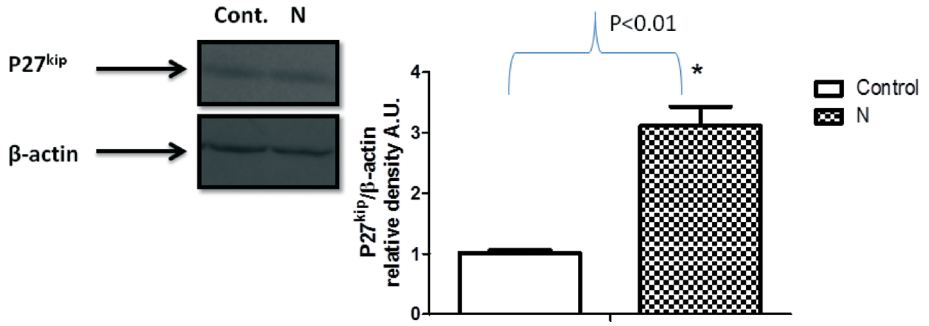

Fig. 6 The effect of compound **11a** (N) on the protein expression of $p27^{kip1}$ in A549 cells assessed through Western blotting. Data are mean ± SD (n = 3). Experiments were carried out in triplicate.

aqueous solubility. The hepatotoxicity score predicts the hepatotoxic nature of the chemical compounds. The ADME. HEPATOTOX.PROB values of most of the compounds lie in the range of 0.93–0.98. Hence, the compounds are likely to possess hepatotoxicity, except for two compounds both containing a cyclohexyl ring instead of a phenyl one. Further studies are necessary to determine the hepatotoxic dose levels. Score predicts the hepatotoxic nature of the studied chemical compound through its effect on CYP2D6 score. More than half of the compounds are predicted as non-inhibitors of CYP2D6, so the results are reliable. Hence, the side effects (*i.e.* liver dysfunction) are not expected upon administration of these compounds. The plasma protein binding model predicts whether a compound is likely to be highly bound to carrier proteins in the blood. There is a high probability that these compounds can reach the desired targets as all of the compounds showed more than 95% plasma protein binding.

PSA is a key property that has been linked to drug bioavailability. Thus, passively absorbed molecules with PSA >140 are thought to have low bioavailability. All the synthesized compounds have PSA ranging from 60.87–94.86, thus they theoretically should present good passive oral absorption.

2.5. Final conclusion

In this study, we have designed and synthesized a novel series of pyrazolo[3,4-*d*]pyrimidine derivatives and tested their activity against VEGFR-2.

Biological evaluation revealed that compound **11a** displayed significant activity on an NCI 60-cell panel. It showed high specificity against CNS cancer, and moderate specificity against NSCLC, ovarian and renal cancer cell lines. Further investigation showed that compound **11a** induced cell cycle arrest at G0/G1 phase and this could be at least partly due to its ability to downregulate cyclin D1 and upregulate $p27^{kip1}$ levels.

Also, compounds **3b**, **d** and **e**, **7d**, **9b**, **11b**, and **11f** showed high antiproliferative activity against the MCF-7 breast cancer cell line.

On the other hand, compounds **3b**, **7a**, and **11b** showed weak inhibition against Aurora-A, EGFR, and PDGFR kinases, respectively.

The structures of the weak inhibitors will be optimized to achieve optimum binding through SAR studies and hence, the activity will be enhanced. Such modification may involve insertion of a methylene group between the aryl moiety and N-1 of pyrazolopyrimidine to render the molecule more flexible to accommodate better fitting with the target enzyme. This suggested modification was based on the fact that the cyclohexylamide derivative displayed the highest activity.

However, the exact inhibitory mechanism of these compounds could not be fully described but is still a subject for future investigation.

3 Experimental

3.1. Chemistry

The starting materials and reagents were purchased from Sigma-Aldrich and Alfa-Aesar Organics and used without further purification. Melting points were determined on a Stuart Scientific apparatus and uncorrected reactions were monitored using thin layer chromatography (TLC) performed on 0.255 mm silica gel plates with visualization under UV light (254 nm). FT-IR spectra were recorded on a Perkin-Elmer spectrophotometer using KBr discs. ^{1}H-NMR spectra were recorded on a Perkin-Elmer 300 MHz spectrometer in δ scale (ppm) and J (Hz) using TMS as the standard signal at Professor Dr. Ahmed Farag's Laboratory at Cairo University. ^{13}C-NMR spectra were recorded on a Perkin-Elmer 400 MHz spectrometer in δ scale (ppm) at the NMR Center of the Faculty of Pharmacy, Cairo University. EI-MS spectra were recorded on a Finnigan Mat SSQ 7000 (70 eV) mass spectrometer at the Microanalytical Center at Cairo University. Elemental analysis was performed at the Microanalytical Center at Al-azhar University.

The reported intermediates **1a** and **b** as well as **2a** and **b** were synthesized according to the reported experimental procedures.

General procedure for the preparation of 1-(substituted phenyl)-3-(4-((1-substituted phenyl-1*H*-pyrazolo[3,4-*d*]pyrimidin-4-yl)amino)phenyl)urea (3a–e). To a solution of 1-(4-aminophenyl)-

Table 3 Cytotoxic activity of the synthesized compounds (**3a–e**, **4a** and **b**, **7b–e**, **9b** and **d**, **11b–f**, and **13b–d**)

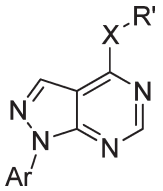

Entry	Compoundcode	R	X	R′	IC_{50} (μM)on MCF-7[a]
1	**3a**	Ph	NH	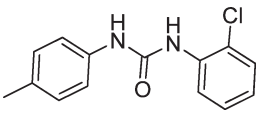	55.07
2	**3b**	Ph	NH	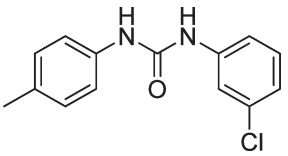	4.20
3	**3c**	Ph	NH	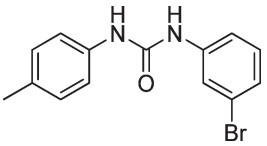	36.33
4	**3d**	*p*-Chlorophenyl	NH	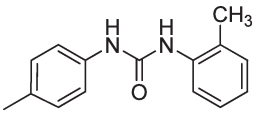	3.15
5	**3e**	*p*-Chlorophenyl	NH	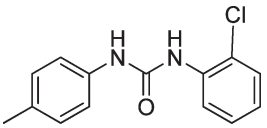	9.05
6	**4a**	Ph	O	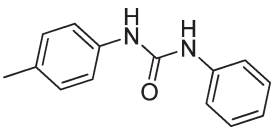	>100
7	**4b**	*p*-Chlorophenyl	O	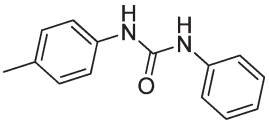	82.53
8	**7b**	Ph	NH	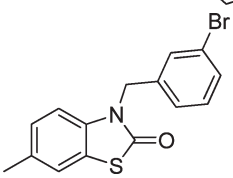	46.06
9	**7c**	Ph	NH	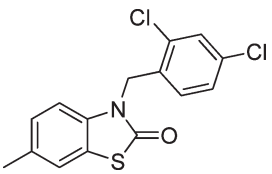	44.04
10	**7d**	Ph	NH	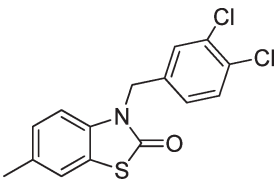	1.60
11	**7e**	*p*-Chlorophenyl	NH	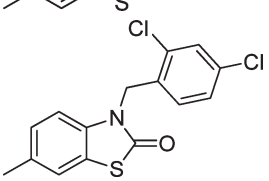	>100

Table 3 *(continued)*

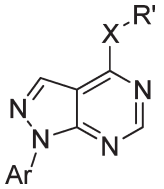

Entry	Compoundcode	R	X	R′	IC_{50} (μM)on MCF-7[a]
12	**9b**	Ph	NH	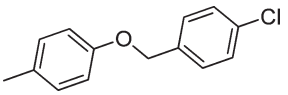	4.36
13	**9d**	*p*-Chlorophenyl	NH	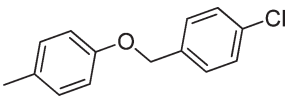	>100
14	**11b**	Ph	NH	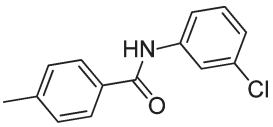	1.12
15	**11c**	Ph	NH	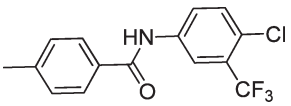	75.87
16	**11d**	*p*-Chlorophenyl	NH	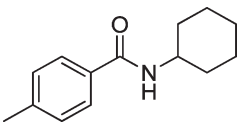	>100
17	**11e**	*p*-Chlorophenyl	NH	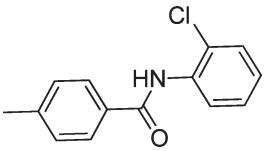	>100
18	**11f**	*p*-Chlorophenyl	NH	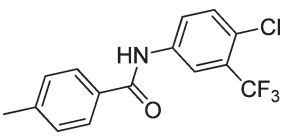	4.92
19	**13b**	Ph	NH	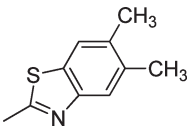	>100
20	**13c**	Ph	NH	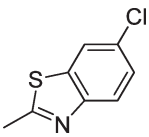	>100
21	**13d**	*p*-Chlorophenyl	NH	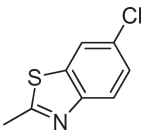	85.59
22	Doxorubicin				1.172

[a] The values given are means of three experiments.

3-substituted phenylurea (3 mmol) in ethanol (20 ml), an equimolar amount of 4-chloro-1-(4-substituted phenyl)-1*H*-pyrazolo[3,4-*d*]pyrimidine (**1a** and **b**) was added followed by addition of 0.2 ml of triethylamine and the mixture was heated under reflux for 18 h. The reaction mixture was monitored by TLC till completion of the reaction. The reaction mixture was then filtered while hot and the precipitate was crystallized from an ethanol/water mixture to give the target compounds **3a–e**.

*1-(2-Chlorophenyl)-3-(4-((1-phenyl-1H-pyrazolo[3,4-d]pyrimidin-4-yl)amino)phenyl)urea (**3a**).* Yield 54.31%; m.p. >280 °C; FT-IR

Table 4 Computer-aided ADMET screening results of the synthesized compounds

CPD ID	BBB_Lev[a]	Absorp_Lev[b]	AQ SOl LEV[c]	Hepatox[d]	Hepatox Prob	CYP2D6[e]	PPB_Lev[f]	*A* log *P*98	Unk_*A* log *P*98	ADEM_PSA_2D[g]
3a	4	1	1	1	0.966	0	2	4.983	0	94.862
3b	4	1	1	1	0.96	0	2	4.983	0	94.862
3c	4	1	1	1	0.96	1	2	5.067	0	94.862
3d	4	1	1	1	0.953	1	2	5.496	0	94.862
3e	4	1	1	1	0.966	0	2	5.647	0	94.862
4a	4	0	2	1	0.96	1	2	4.329	0	90.982
4b	4	1	1	1	0.96	1	2	4.993	0	90.982
7a	4	1	1	1	0.993	0	2	6.148	0	72.594
7b	4	2	1	1	0.993	0	2	6.232	0	72.594
7c	4	2	0	1	0.993	0	2	6.812	0	72.594
7d	4	2	0	1	0.993	0	2	6.812	0	72.594
7e	4	3	0	1	0.986	0	2	7.477	0	72.594
9a	1	0	1	1	0.986	1	2	5.193	0	60.871
9b	1	1	1	1	0.986	1	2	5.857	0	60.871
9c	1	1	1	1	0.986	1	2	5.857	0	60.871
9d	4	2	1	1	0.986	1	2	6.522	0	60.871
11a	2	0	1	0	0.311	1	2	4.692	0	82.052
11b	4	0	1	1	0.973	1	2	5.075	0	82.052
11c	4	2	1	1	0.933	0	2	6.017	0	82.052
11d	4	1	1	0	0.337	0	2	5.356	0	82.052
11e	4	1	1	1	0.966	1	2	5.739	0	82.052
11f	4	2	0	1	0.98	0	2	6.682	0	82.052
13a	1	0	1	1	0.993	0	2	5.068	0	63.202
13b	1	0	1	1	0.887	1	2	5.554	0	63.202
13c	1	0	1	1	0.986	0	2	5.246	0	63.202
13d	4	1	0	1	0.986	0	2	5.91	0	63.202

[a] BBB_Level; 4 = undefined, 2 = medium penetration, 1 = high penetration. [b] Absorp_Level; 3 = very low absorption, 2 = low absorption, 1 = moderate absorption, 0 = good absorption. [c] AQ SOl LEV; 2 = low solubility, 1 = very low but soluble, 0 = extremely low solubility. [d] Hepatotox_Level; 1 = toxic, 0 = non-toxic. [e] CYP 2D6; 1 = likely to inhibit, 0 = non-inhibitor. [f] PPB (plasma protein binding); 2 = more than 95%, 1 = more than 90%, 0 = less than 90%. [g] PSA (polar surface area); cpds must have log *P* value not greater than 5.0 to attain a reasonable probability of being well absorbed.

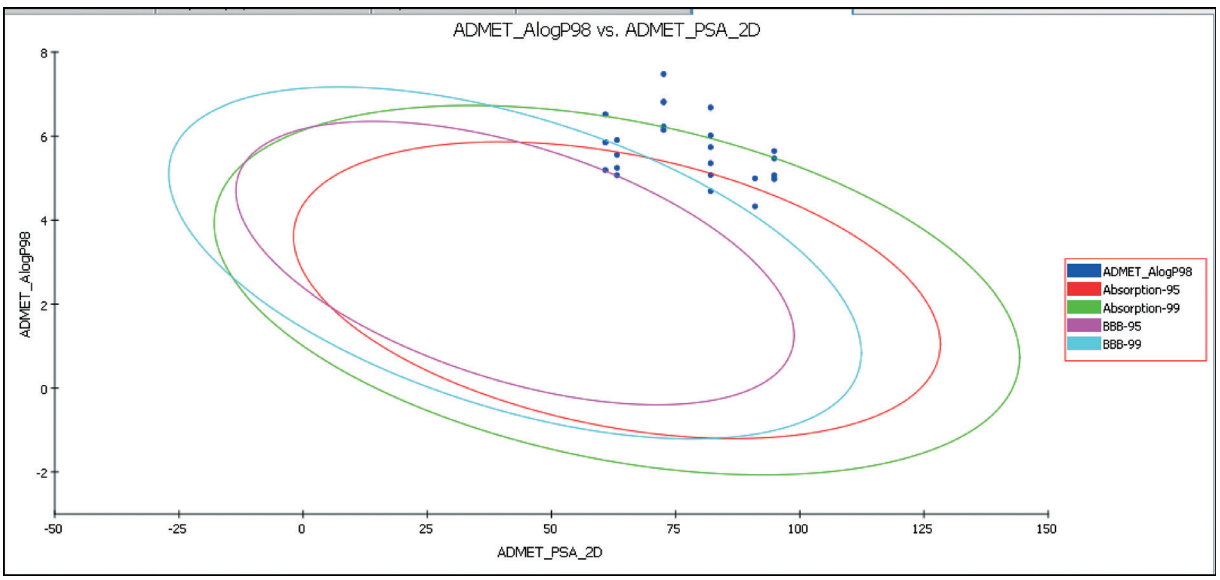

Fig. 7 Human intestinal absorption (HIA) and blood brain barrier plot for the newly synthesized compounds.

(ν max, cm^{-1}): 3310 (NH), 1705 (C═O amide), 1630 (C═N); ^{1}H-NMR (300 MHz, DMSO-d_6): δ ppm 10.15 (s, 1H, NH, D_2O exchangeable), 9.44 (s, 1H, NH, D_2O exchangeable), 8.50 (s, 2H, heterocyclic H), 8.30 (s, 1H, NH, D_2O exchangeable), 8.23–8.17 (m, 3H, ArH), 7.75 (d, J = 7.3 Hz, 2H, ArH), 7.59–7.44 (m, 5H, ArH), 7.39–7.33 (m, 2H, ArH), 7.03 (t, J = 7.5 Hz, 1H, ArH); MS (Mwt.: 455.13): m/z (% rel. int.) 457.00 (M^+ + 2, 10.28), 456.00 (M^+ + 1, 8.4), 455.00 (M^+, 32.12), 328.05

(74.97), 302.05 (100); Anal. calcd for $C_{24}H_{18}ClN_7O$: C, 63.23; H, 3.98; N, 21.51; found: C, 63.41; H, 3.96; N, 21.63.

The analytical characterization data for compounds **3b–e** are provided in the ESI.‡

General procedure for the preparation of 1-substituted phenyl-3-(4-((1-phenyl-1*H*-pyrazolo[3,4-*d*]pyrimidin-4-yl)oxy)phenyl)urea (4a and b). To a solution of 1-(4-hydroxyphenyl)-3-phenylurea (3 mmol) in acetonitrile (20 ml), an equimolar amount of 4-chloro-1-(4-substituted phenyl)-1*H*-pyrazolo[3,4-*d*]pyrimidine was added. A catalytic amount of cesium carbonate was added to the mixture which was then heated under reflux overnight. The reaction mixture was then filtered while hot and the precipitate was crystallized from an ethanol/water mixture to give the target compounds **4a** and **b**.

*1-Phenyl-3-(4-((1-phenyl-1H-pyrazolo[3,4-d]pyrimidin-4-yl)oxy)phenyl)urea (**4a**).* Yield 23%; m.p. >300 °C; FT-IR (ν max, cm^{-1}): 3315 (NH), 1675 (C═O), 1630 (C═N); ^{1}H-NMR (300 MHz, DMSO-d_6): δ ppm 8.80 (s, 1H, NH, D_2O exchangeable), 8.70 (s, 1H, NH, D_2O exchangeable), 8.66 (s, 1H, heterocyclic H), 8.41 (s, 1H, heterocyclic H), 8.18 (d, J = 7.4 Hz, 2H, ArH), 7.63–7.56 (m, 4H, ArH), 7.48–7.42 (m, 3H, ArH), 7.31–7.27 (m, 4H, ArH), 6.99 (t, J = 6.0 Hz, 1H, ArH); ^{13}C-NMR (400 MHz, DMSO-d_6): 164.10, 156.41, 155.18, 153.07, 146.68, 140.12, 138.73, 138.27, 133.69, 129.86, 129.27, 127.49, 122.68, 122.36, 121.65, 119.88, 118.73, 104.09; MS (Mwt.: 422.44): m/z (% rel. int.) 423.20 (M^+ + 1, 4.14), 422.20 (M^+, 14.05), 329.10 (45.17), 303.15 (78.97), 93.10 (100); Anal. calcd for $C_{24}H_{18}N_6O_2$: C, 68.24; H, 4.29; N, 19.89; found: C, 68.27; H, 4.34; N, 20.14.

*1-(4-((1-(4-Chlorophenyl)-1H-pyrazolo[3,4-d]pyrimidin-4-yl)oxy)phenyl)-3-phenylurea (**4b**).* Yield 16%; m.p. charring at 230 °C; FT-IR (ν max, cm^{-1}): 3300 (NH), 1675 (C═O), 1625 (C═N); ^{1}H-NMR (300 MHz, DMSO-d_6): δ ppm 10.37 (s, 1H, NH, D_2O exchangeable), 9.30 (s, 1H, NH, D_2O exchangeable), 8.69 (s, 1H, heterocyclic H), 8.36 (s, 1H, heterocyclic H), 8.25 (d, J = 7.4 Hz, 2H, ArH), 7.69–7.64 (m, 4H, ArH), 7.55 (d, J = 6.0 Hz, 2H, ArH), 7.27–7.19 (m, 4H, ArH), 6.91 (t, J = 6.0 Hz, 1H, ArH); MS (Mwt.: 456.11): m/z (% rel. int.) 458.10 (M^+ + 1, 10.64), 456.10 (M^+, 32.15), 366.10 (41.23), 93.10 (100); Anal. calcd for $C_{24}H_{17}ClN_6O_2$: C, 63.09; H, 3.75; N, 18.39; found: C, 63.17; H, 3.79; N, 18.51.

General procedure for the preparation of 3-substituted benzyl-6-nitro-2,3-dihydrobenzo[*d*]thiazol-2-one (5a–d). To a stirred solution of 6-nitro-3*H*-benzothiazol-2-one (2.943 g, 15 mmol) in acetone (22.5 ml), water (0.75 ml) and 85% KOH (0.99 g, 30 mmol) were added followed by addition of the appropriate substituted benzyl chloride (15 mmol) in one portion. The reaction mixture was refluxed for 24 h, then cooled to 5 °C after which 60 g of ice-cold water was added and the mixture was stirred at 0–10 °C for 1 h. The obtained solid was filtered, washed with cold water and diethyl ether, dried at room temperature and crystallized from acetone/water to give pure compounds **5a–d**. **5a**: R_2 = 4-Cl; yield 95.5%; m.p. 110–112 °C. **5b**: R_2 = 2,4-diCl; yield 90%; m.p. 136–137 °C. **5c**: R_2 = 3,4-diCl; yield 92%; m.p. 142–146 °C. **5d**: R_2 = 3-Br; yield 80%; m.p. 119–120 °C.

General procedure for the preparation of 3-substituted benzyl-6-amino-2,3-dihydrobenzo[*d*]thiazol-2-one (6a–d). To a solution of appropriate 3-substituted benzyl-6-amino-2,3-dihydrobenzo[*d*]thiazol-2-one (**5a–d**, 5 mmol) in an ethanol/THF mixture (3 : 1, 100 ml), 10% Pd/C (0.2 g) was added and the mixture was hydrogenated in a bar-shaker hydrogenator at 35 psi and room temperature for 6 h. The mixture was filtered through celite and the filtrate was concentrated to give crude amines which were then crystallized from diethyl ether to yield pure crystals of compounds **6a–d**. **6a**: R_2 = 4-Cl; yield 87.7%; m.p. 123–127 °C. **6b**: R_2 = 2,4-diCl; yield 99%; m.p. 150–155 °C. **6c**: R_2 = 3,4-diCl; yield 95%; m.p. 157–158 °C. **6d**: R_2 = 3-Br; yield 82%; m.p. 135–137 °C.

General procedure for the preparation of 6-((1-(4-substituted phenyl)-1*H*-pyrazolo[3,4-*d*]pyrimidin-4-yl)amino)-3-(substituted benzyl)benzo[*d*]thiazol-2(3*H*)-one (7a–e). To a solution of 6-amino-3-(substituted benzyl)benzo[*d*]thiazol-2(3*H*)-one (**6a–d**, 3 mmol) in ethanol (20 ml), an equimolar amount of 4-chloro-1-(4-substituted phenyl)-1*H*-pyrazolo[3,4-*d*]pyrimidine (**1a** and **b**) was added after which 0.2 ml of triethylamine was added and the mixture was stirred under reflux for 25 h. The reaction mixture was then filtered while hot and the precipitate was crystallized from an ethanol/water mixture to give the target compounds **7a–e**.

*3-(4-Chlorobenzyl)-6-((1-phenyl-1H-pyrazolo[3,4-d]pyrimidin-4-yl)amino)benzo[d]thiazol-2(3H)-one (**7a**).* Yield 55.4%; m.p. 200 °C; FT-IR (ν max, cm^{-1}): 3300 (NH), 1690 (C═O), 1640 (C═N); ^{1}H-NMR (300 MHz, DMSO-d_6): δ ppm 10.29 (s, 1H, NH, D_2O exchangeable), 8.51 (s, 2H, heterocyclic H), 8.27 (s, 1H, ArH), 8.19 (d, J = 7.4 Hz, 2H, ArH), 7.59–7.54 (m, 3H, ArH), 7.45–7.35 (m, 5H, ArH), 7.32 (d, J = 7.3 Hz, 1H, ArH), 5.20 (s, 2H, aliphatic CH_2); MS (Mwt.: 484.96): m/z (% rel. int.) 486.05 (M^+ + 2, 27.08), 485.05 (M^+ + 1, 21.97), 484.05 (M^+, 66.38), 359.05 (78.12), 125 (100); Anal. calcd for $C_{25}H_{17}ClN_6OS$: C, 61.92; H, 3.53; N, 17.33; found: C, 62.07; H, 3.59; N, 17.48.

The analytical characterization data for compounds **7b–e** are provided in the ESI.‡

General procedure for the preparation of 4-((4-substituted benzyl)oxy)aniline (8a and b). A 4-nitrophenyl substituted benzyl ether derivative (17.4 mmol) was dissolved in ethanol (50 ml) before adding stannous chloride dihydrate (19.04 g, 84.4 mmol). The mixture was stirred under reflux for 4 h. The reaction was monitored by TLC using dichloromethane as an eluent. After completion of the reaction, the solvent was evaporated under vacuum and the mixture was treated with a concentrated aqueous solution of sodium bicarbonate until the effervescence ceased. The reaction mixture was then extracted with ethyl acetate (4 × 50 ml), and the organic layers were collected, dried over anhydrous sodium sulfate, filtered and evaporated to dryness. The obtained residue was crystallized from methanol to give **8a** and **b**. **8a**: R_3 = H; yield 97%; m.p. 44–45 °C. **8b**: R_3 = Cl; yield 71%; m.p. 106–108 °C.

General procedure for the preparation of *N*-(4-((4-substituted benzyl)oxy)phenyl)-1-(4-substituted phenyl)-1*H*-pyrazolo[3,4-*d*]pyrimidin-4-amine (9a–d). To a solution of

4-((4-substituted benzyl)oxy)aniline (**8a** and **b**, 3 mmol) in ethanol (20 ml), an equimolar amount of 4-chloro-1-(4-substituted phenyl)-1*H*-pyrazolo[3,4-*d*]pyrimidine (**1a** and **b**) was added followed by the addition of 0.2 ml of triethylamine and the mixture was stirred under reflux for 48 h. It was followed by TLC till completion of the reaction. The reaction mixture was then filtered while hot and the precipitate was crystallized from an ethanol/water mixture to give the target compounds **9a–d**.

*N-(4-(Benzyloxy)phenyl)-1-phenyl-1H-pyrazolo[3,4-d]pyrimidin-4-amine (**9a**).* Yield 35%; m.p. 190–192 °C; FT-IR (ν max, cm^{-1}): 3290 (NH), 1610 (C═O), 1640 (C═N); ^{1}H-NMR (300 MHz, DMSO-d_6): δ ppm 10.09 (s, 1H, NH, D_2O exchangeable), 8.46 (s, 2H, heterocyclic H), 8.20 (d, J = 6.0 Hz, 2H, ArH), 7.69 (d, J = 7.6 Hz, 2H, ArH), 7.55 (t, J = 6.0 Hz, 2H, ArH), 7.48–7.33 (m, 6 H, ArH), 7.08 (d, J = 7.6 Hz, 2H, ArH), 5.13 (s, 2H, aliphatic CH_2); MS (Mwt.: 393.44): m/z (% rel. int.) 394.15 (M^+ + 1, 38.16), 393.25 (M^+, 50.03), 302.15 (100), 91.05 (69.89); Anal. calcd for $C_{24}H_{19}N_5O$: C, 73.27; H, 4.87; N, 17.80; found: C, 73.39; H, 4.84; N, 17.96.

The analytical characterization data for compounds **9b–d** are provided in the ESI.‡

General procedure for the preparation of 4-amino-*N*-substituted benzamide (10a–d). Stannous chloride dihydrate (0.39 g, 1.76 mmol) was added to a solution of *N*-substituted-4-nitrobenzamide (**9a–d**, 0.59 mmol) in ethanol (8 ml) and the reaction mixture was stirred under reflux for 3 h. The resulting mixture was partitioned between ethyl acetate (50 ml) and an aqueous solution of sodium carbonate (5%, 30 ml); the organic layer was separated, washed with brine (30 ml), dried over anhydrous sodium sulfate, filtered and evaporated under reduced pressure. The crude residue was purified by crystallization using hexane/EtOAc to yield pure title compounds **10a–d**. **10a**: R_4 = cyclohexyl; yield 82%; m.p. 183–184 °C. **10b**: R_4 = 3-chlorophenyl; yield 86%; m.p. 142–144 °C. **10c**: R_4 = 2-chlorophenyl; yield 88%; m.p. 159–160 °C. **10d**: R_4 = 4-chloro-3-CF_3phenyl; yield 44%; m.p. 178–180 °C.

General procedure for the preparation of *N*-substituted-4-((1-(4-substituted phenyl)-1*H*-pyrazolo[3,4-*d*]pyrimidin-4-yl)amino)benzamide (11a–f). To a solution of 4-amino-*N*-chlorobenzamide (**10a–d**, 3 mmol) in ethanol (20 ml), an equimolar amount of 4-chloro-1-(4-substituted phenyl)-1*H*-pyrazolo[3,4-*d*]pyrimidine (**1a** and **b**) was added after which 0.2 ml of triethylamine was added and the mixture was then stirred under reflux for 72 h. The reaction mixture was filtered while hot and the precipitate was crystallized from an ethanol/water mixture to give the target compounds **11a–f**.

*N-Cyclohexyl-4-((1-phenyl-1H-pyrazolo[3,4-d]pyrimidin-4-yl)amino)benzamide (**11a**).* Yield 67.3%; m.p. 272–273 °C; FT-IR (ν max, cm^{-1}): 2975 (aliphatic CH), 3310 (NH), 1705 (C═O), 1670 (C═N); ^{1}H-NMR (300 MHz, DMSO-d_6): δ ppm 10.38 (s, 1H, NH, D_2O exchangeable), 8.61 (s, 2H, heterocyclic H), 8.21 (d, J = 7.6 Hz, 2H, ArH), 7.93 (dd, J = 6.0, 1.8 Hz, 4H, ArH), 7.58 (t, J = 6.0 Hz, 2H, ArH), 7.37 (t, J = 6.0 Hz, 1H, ArH), 3.78 (p, 1H, NH–CH–$(CH_2)_2$), 1.82–1.59 (m, 6H, cyclohexyl), 1.31 (p, 4H, cyclohexyl); ^{13}C-NMR (400 MHz, DMSO-d_6): 165.29, 156.50, 154.76, 153.52, 141.92, 139.14, 134.20, 130.01, 129.69, 128.54, 126.91, 121.30, 120.43, 103.23, 48.76, 32.98, 25.77, 25.46; MS (Mwt.: 412.49): m/z (% rel. int.) 413.15 (M^+ + 1, 14.30), 412.15 (M^+, 49.23), 329.10 (100), 314.05 (72.52); Anal. calcd for $C_{24}H_{24}N_6O$: C, 69.88; H, 5.86; N, 20.37; found: C, 70.03; H, 5.84; N, 20.45.

The analytical characterization data for compounds **11b–f** are provided in the ESI.‡

General procedure for the preparation of 5,6-disubstituted-*N*-(1-(4-substituted phenyl)-1*H*-pyrazolo[3,4-*d*]pyrimidin-4-yl)benzo[*d*]thiazol-2-amine (13a–d). To a solution of 5,6-disubstituted-benzo[*d*]thiazol-2-amine (**12a–c**, 5 mmol) in ethanol (20 ml), an equimolar amount of 4-chloro-1-(4-substituted phenyl)-1*H*-pyrazolo[3,4-*d*]pyrimidine (**1a** and **b**) was added after which 0.2 ml of triethylamine was added to the mixture which was then stirred under reflux for 48 h. The reaction was monitored by TLC till the reaction was finished. Then, the reaction mixture was filtered while hot and the precipitate was crystallized from an ethanol/water mixture to give the target compounds **13a–d**.

*6-Methyl-N-(1-phenyl-1H-pyrazolo[3,4-d]pyrimidin-4-yl)benzo[d]thiazol-2-amine (**13a**).* Yield 21.3%; m.p. >250 °C; FT-IR (ν max, cm^{-1}): 3310 (N–H), 2985 (aliphatic CH), 1680 (C═N); ^{1}H-NMR (300 MHz, DMSO-d_6): δ ppm 12.82 (s, 1H, NH, D_2O exchangeable), 8.78 (s, 2H, heterocyclic H), 8.20 (d, J = 6.0 Hz, 2H, ArH), 7.78 (s, 1H, ArH), 7.69–7.55 (m, 3H, ArH), 7.40 (t, J = 6.0 Hz, 1H, ArH), 7.27 (d, J = 6.0 Hz, 1H, ArH), 2.37 (s, 3H, aliphatic CH_3); ^{13}C-NMR (400 MHz, DMSO-d_6): 155.32, 153.45, 138.93, 134.49, 133.17, 132.68, 129.73, 127.89, 127.16, 121.59, 121.51, 103.40, 21.49; MS (Mwt.: 358.42): m/z (% rel. int.) 360.10 (M^+ + 2, 5.59), 359.05 (M^+ + 1, 17.01), 358.15 (M^+, 61.98), 77.05 (100); Anal. calcd for $C_{19}H_{14}N_6S$: C, 63.67; H, 3.94; N, 23.45; found: C, 63.81; H, 3.87; N, 23.55.

The analytical characterization data for compounds **13b–d** are provided in the ESI.‡

3.2. Biological evaluation

3.2.1. Enzyme inhibition assay. The determination of *in vitro* enzyme inhibition for the synthesized compounds was carried out in KINEXUS Corporation, Vancouver, British Columbia, Canada. Kinexus uses a radioactive assay format for profiling evaluation of protein kinase targets and all assays were performed in a designated radioactive working area. Protein kinase assays were carried out at ambient temperature for 30 minutes (depending on the target) in a final volume of 25 μL according to the following assay reaction receipt: 5 μL of diluted active protein kinase target (~10–50 nM final protein concentration in the assay), 5 μL of peptide substrate, 5 μL of kinase assay buffer, 5 μL of compound (various concentrations) and 5 μL of ^{28}P-ATP (250 μM stock solution).

The assay was initiated by the addition of ^{28}P-ATP and the reaction mixture was incubated at 30 °C for 20–40 minutes depending on the protein kinase target. After the incubation period, the assay was terminated by spotting 10 μL of the

reaction mixture onto a multiscreen phosphocellulose P81 plate. The multiscreen phosphocellulose P81 plate was washed 3 times for approximately 15 minutes each in 1% phosphoric acid solution. The radioactivity on the P81 plate was counted in the presence of scintillation fluid in a TriLux scintillation counter. A blank control was set up for each protein kinase target, which included all the assay components except the appropriate substrate (replaced with an equal volume of kinase assay buffer). The corrected activity for the protein kinase target was determined by removing the blank control value.[40]

3.2.2. Antitumor activity screening

3.2.2.1. Screening at NIH, Bethesda, Maryland, USA. The cytotoxicity of the synthesized compounds was assayed using the standardized assay procedure of the National Cancer Institute (NCI Bethesda, Maryland, USA).[41]

3.2.2.2. Cell culture. The experimental procedure of cell culture assay is provided in the ESI.‡

3.2.2.3. SRB cytotoxicity assay. SRB assay was performed according to the reported procedure[42] and the experimental part is provided in the ESI.‡

3.2.2.4. DNA-flow cytometry analysis. A549 cells at a density of 2×10^5 cells were exposed to the tested compounds at their IC_{50} concentration for 48 h. The cells were collected by trypsinization, washed in PBS and then fixed in ice-cold absolute alcohol. Thereafter, cells were stained using a CycleTEST™ PLUS DNA reagent kit (BD Biosciences, San Jose, CA) according to the manufacturer's instructions. Cell cycle distribution was determined using a FACSCalibur flow cytometer (BD Biosciences, San Jose, CA).[43]

3.2.2.5. Immunocytochemistry. A549 cells were seeded on ibidi® 12-well slide μ-chamber (Munich, Germany) at a density of 2×10^5 cells per mL. After exposure to different treatments, cells were fixed with 70% ethanol. Then, the cells were washed in phosphate buffered saline (PBS) and incubated with 0.01% Triton X-100 in PBS for 1 min to permeabilize the cell membranes. The cells were afterwards incubated with 0.3% H_2O_2 in PBS for 20 min to quench endogenous peroxidase activity and then in 5% normal horse serum in Tris-buffered saline plus Tween-20 (TBST) for 30 min to block the non-specific binding of the secondary antibody. Thereafter, the cells were incubated overnight with primary specific antibodies (rabbit monoclonal for cyclin D1; dilution of 1 : 100; Cell Signaling, Danvers, MA). In the following day, the slides were incubated with the corresponding conjugated anti-rabbit or anti-mouse IgG (dilution of 1 : 2000; Cell Signaling, Danvers, MA). The cells were treated afterwards with streptavidin horseradish peroxidase complex (dilution of 1 : 100; ABC/HRP; Vector Laboratories, Burlingame, CA, USA) in TBST for 50 min. The color of the reaction was developed for 5 min in 3,30-diaminobenzidine (DAB) solution (Santa Cruz Biotechnology, Dallas, TX). The percentage of DAB-positive cells per high power field was calculated by [number of DAB-positive cells/total number of cells] × 100.[43]

3.2.2.6. Western blot analysis. A primary antibody against $p27^{kip1}$ (Cell Signaling, Danvers, MA) was used to assess the protein expression of this marker in the tested cells according to the reported procedure[43] and the experimental part is provided in the ESI.‡

Author contribution

MFT designed and performed cell culture studies, flow cytometry, western blotting and immunocytochemistry experiments as well as data analysis and writing. AE performed SRB–MCF-7 cytotoxicity screening.

Acknowledgements

The authors would like to thank the Science and Technology Development Fund (STDF) for funding the center for drug discovery and development research at the Faculty of Pharmacy Ain Shams University (Project No. 5251) and for partial funding of this study. The authors are also grateful for the National Cancer Institute (NCI), Bethesda, Maryland, USA, for performing the *in vitro* anticancer testing for the selected compounds over their panel of cell lines.

References

1 "American Cancer Society: Cancer Facts and Figures 2012. American Cancer Society: Atlanta, 2012.".
2 Y. L. Chen, S. Z. Lin, J. Y. Chang, Y. L. Cheng, N. M. Tsai, S. P. Chen, W. L. Chang and H. J. Harn, *Biochem. Pharmacol.*, 2006, **72**, 308.
3 M. Nakhjiri, M. Safavi, E. Alipour, S. Emami, A. F. Atash, M. Jafari-Zavareh, S. K. Ardestani, M. Khoshneviszadeh, A. Foroumadi and A. Shafiee, *Eur. J. Med. Chem.*, 2012, **50**, 113.
4 M. K. Abd El Hamid, M. D. Mihovilovic and H. B. El-Nassan, *Eur. J. Med. Chem.*, 2012, **57**, 323.
5 H. A. F. Toque, F. B. M. Priviero, C. E. Texeira, E. Perissutti, F. Fiorino, B. Severino, F. Frecentese, R. Lorenzetti, J. S. Baracat and V. Santagada, *J. Med. Chem.*, 2008, **51**, 2807.
6 R. J. Gillespie, I. A. Cliffe, C. E. Dawson, C. T. Dourish, S. Gaur, A. M. Jordan, A. R. Knight, J. Lerpiniere, A. Misra and R. M. Pratt, *Bioorg. Med. Chem. Lett.*, 2008, **18**, 2924.
7 E. R. El-Bendary and F. A. Badria, *Arch. Pharm.*, 2000, **333**, 99.
8 J. L. Rideout, T. A. Krenitsky, G. W. Koszalka, N. K. Cohn, E. Y. Chao, G. B. Elion, V. S. Latter and R. B. Williams, *J. Med. Chem.*, 1982, **25**, 1040.
9 A. Ali, G. E. Taylor, K. Ellsworth, G. Harris, R. Painter, L. Lynn and K. Young, *J. Med. Chem.*, 2003, **46**, 1824.
10 X. J. Song, Y. Shao and X. G. Dong, *Chin. Chem. Lett.*, 2011, **22**, 1036.
11 A. Kumar, I. Ahmad, B. S. Chhikara, R. Tiwari, D. Mandal and K. Parang, *Bioorg. Med. Chem. Lett.*, 2011, **21**, 1342.
12 A. J. Garton, A. P. Crew, M. Franklin, A. R. Cooke, G. M. Wynne, L. Castaldo, J. Kahler, S. L. Winski, A. Franks, E. N. Brown, M. A. Bittner, J. F. Keily, P. Briner, C. Hidden, M. C. Srebernak, C. Pirrit, M. O'Connor, A. Chan, B. Vulevic, D. Henninger, K. Hart, R. Sennello, A. H. Li, T. Zhang, F. Richardson, D. L. Emerson, A. L. Castelhano, L. D. Arnold and N. W. Gibson, *Cancer Res.*, 2006, **66**, 1015.

13 G. Martiny-Baron, P. Holzer, E. Billy, C. Schnell, J. Brueggen, M. Ferretti, N. Schmiedeberg, J. M. Wood, P. Furet and P. Imbach, *Angiogenesis*, 2010, **13**, 259.
14 R. Li and J. A. Stafford, "*Kinase Inhibitor Drugs*", John Wiley & Sons, Hoboken, 1st edn, 2009, DOI: 10.1002/9780470524961.
15 E. M. Berge, D. W. Bowles, T. W. Flaig, E. T. Lam and A. Jimeno, *Drugs Today*, 2013, **49**, 303.
16 A. C. Dar and K. M. Shokat, *Annu. Rev. Biochem.*, 2011, **80**, 769.
17 K. Kubo, T. Shimizu, S. Ohyama, H. Murooka, A. Iwai, K. Nakamura, K. Hasegawa, Y. Kobayashi, N. Takahashi, K. Takahashi, S. Kato, T. Izawa and T. Isoe, *J. Med. Chem.*, 2005, **48**, 1359.
18 C. E. Whittles, T. M. Pocock, S. R. Wedge, J. Kendrew, L. F. Hennequin, S. J. Harper and D. O. Bates, *Microcirculation*, 2002, **9**, 513.
19 H. Huynh, V. C. Ngo, J. Fargnoli, M. Ayers, K. C. Soo, H. N. Koong, C. H. Thng, H. S. Ong, A. Chung, P. Chow, P. Pollock, S. Byron and E. Tran, *Clin. Cancer Res.*, 2008, **14**, 6146.
20 S. Zhang, Z. Cao, H. Tian, G. Shen, Y. Ma, H. Xie, Y. Liu, C. Zhao, S. Deng, Y. Yang, R. Zheng, W. Li, N. Zhang, S. Liu, W. Wang, L. Dai, S. Shi, L. Cheng, Y. Pan, S. Feng, X. Zhao, H. Deng, S. Yang and Y. Wei, *Clin. Cancer Res.*, 2011, **17**, 4439.
21 V. J. Ram and H. Pandey, *Arch. Pharm.*, 1979, **312**, 703.
22 M. Kopp, J. C. Lancelot, P. Dallemagne and S. Rault, *J. Heterocycl. Chem.*, 2001, **38**, 1045.
23 J. Das, R. V. Moquin, S. Pitt, R. Zhang, D. R. Shen, K. W. McIntyre, K. Gillooly, A. M. Doweyko, J. S. Sack, H. Zhang, S. E. Kiefer, K. Kish, M. McKinnon, J. C. Barrish, J. H. Dodd, G. L. Schieven and K. Leftheris, *Bioorg. Med. Chem. Lett.*, 2008, **18**, 2652.
24 E. M. Dokla, A. H. Mahmoud, M. S. A. Elsayed, A. H. El-Khatib, M. W. Linscheid and K. A. Abouzid, *PLoS One*, 2012, **7**, e49284.
25 Q. M. Malik, S. Ijaz, D. C. Craig and A. C. Try, *Tetrahedron*, 2011, **67**, 5798.
26 D. M. Stout, W. L. Matier, C. Barcelon-Yang, R. D. Reynolds and B. S. Brown, *J. Med. Chem.*, 1985, **28**, 295.
27 A. Rana, N. Siddiqui, S. A. Khan, S. Ehtaishamul Haque and M. A. Bhat, *Eur. J. Med. Chem.*, 2008, **43**, 1114.
28 S. M. Abdelaal, S. B. Kong and L. Bauer, *J. Heterocycl. Chem.*, 1992, **29**, 1069.
29 J. J. D'Amico and F. G. Bollinger, *J. Heterocycl. Chem.*, 1989, **26**, 1245.
30 S. Wang, J. Yan, X. Wang, Z. Yang, F. Lin and T. Zhang, *Eur. J. Med. Chem.*, 2010, **45**, 1250.
31 H. Kakuta, X. Zheng, H. Oda, S. Harada, Y. Sugimoto, K. Sasaki and A. Tai, *J. Med. Chem.*, 2008, **51**, 2400.
32 W. P. Hu, Y. K. Chen, C. C. Liao, H. S. Yu, Y. M. Tsai, S. M. Huang, F. Y. Tsai, H. C. Shen, L. S. Chang and J. J. Wang, *Bioorg. Med. Chem.*, 2010, **18**, 6197.
33 P. Skehan, R. Storeng, D. Scudiero, A. Monks, J. McMahon, D. Vistica, J. T. Warren, H. Bokesch, S. Kenney and M. R. Boyd, *J. Natl. Cancer Inst.*, 1990, **82**, 1107.
34 H. S. Robert, *Nat. Rev. Cancer*, 2006, **6**, 813.
35 S. A. Rostom, *Bioorg. Med. Chem.*, 2006, **14**, 6475.
36 M. Hall and G. Peters, *Adv. Cancer Res.*, 1996, **68**, 67.
37 J. A. Diehl, F. Zindy and C. J. Sherr, *Genes Dev.*, 1997, **11**, 957.
38 R. G. Pestell, C. Albanese, A. T. Reutens, J. E. Segall, R. J. Lee and A. Arnold, *Endocr. Rev.*, 1999, **20**, 501.
39 R. V. Patel, P. K. Patel, P. Kumari, D. P. Rajani and K. H. Chikhalia, *Eur. J. Med. Chem.*, 2012, **53**, 41.
40 C. J. Hastie, H. J. McLauchlan and P. Cohen, *Nat. Protoc.*, 2006, **1**, 968.
41 M. C. Alley, D. A. Scudiero, A. Monks, M. L. Hursey, M. J. Czerwinski, D. L. Fine, B. J. Abbott, J. G. Mayo, R. H. Shoemaker and M. R. Boyd, *Cancer Res.*, 1988, **48**, 589.
42 P. Skehan, R. Storeng, D. Scudiero, A. Monks, J. McMahon, D. Vistica, J. T. Warren, H. Bokesch, S. Kenney and M. R. Boyd, *J. Natl. Cancer Inst.*, 1990b, **82**, 1107.
43 M. F. Tolba, A. Esmat, A. M. Al-Abd, S. S. Azab, A. E. Khalifa, H. A. Mosli, S. Z. Abdel-Rahman and A. B. Abdel-Naim, *IUBMB Life*, 2013, **65**, 716.